




Article

Evaluation and Simulation of the Adsorption Capacity of Octocrylene Sunscreen on Commercial Carbon and Biochar from Spent Coffee Beans

Sandra Andreola Franco da Rocha ¹, Bianca Caroline da Silva Rocha ², Luiz Eduardo Zani de Moraes ², João Marcos Pires Villaça ², Diane Scapin ³, Diego Espirito Santo ³ , Regiane da Silva Gonzalez ⁴, Osvaldo Valarini Junior ⁵  and Ana Paula Peron ^{1,3,*} 

- ¹ Graduate Program in Technological Innovations, Federal Technological University of Paraná, Campo Mourão 87301-899, Paraná, Brazil; sandrashalomcm@hotmail.com
- ² Chemical Engineering Course, Federal Technological University of Paraná, Campo Mourão 87301-899, Paraná, Brazil; biancacarolinerocha@alunos.utfpr.edu.br (B.C.d.S.R.); luizm.2002@alunos.utfpr.edu.br (L.E.Z.d.M.); joaovillaca@alunos.utfpr.edu.br (J.M.P.V.)
- ³ Graduate Program in Environmental Engineering, Federal Technological University of Paraná, Francisco Beltrão 85602-863, Paraná, Brazil; dscapin@casan.com.br (D.S.); dsanto@alunos.utfpr.edu.br (D.E.S.)
- ⁴ Graduate Program in Food Technology, Federal Technological University of Paraná, Campo Mourão 87301-899, Paraná, Brazil; regiane@utfpr.edu.br
- ⁵ Academic Department of Food and Chemical Engineering, Federal Technological University of Paraná, Campo Mourão 87301-899, Paraná, Brazil; osvaldovalarini@utfpr.edu.br
- * Correspondence: anaperon@utfpr.edu.br; Tel.: +55-44-3518-1515



Citation: Rocha, S.A.F.d.; Rocha, B.C.d.S.; Moraes, L.E.Z.d.; Villaça, J.M.P.; Scapin, D.; Santo, D.E.; Gonzalez, R.d.S.; Junior, O.V.; Peron, A.P. Evaluation and Simulation of the Adsorption Capacity of Octocrylene Sunscreen on Commercial Carbon and Biochar from Spent Coffee Beans. *Processes* **2024**, *12*, 1249. <https://doi.org/10.3390/pr12061249>

Academic Editors: Silvia Roman Suero, Suhas, José Castanheiro, Paulo Alexandre Mira Mourão and Isabel Cansado

Received: 22 May 2024

Revised: 10 June 2024

Accepted: 11 June 2024

Published: 18 June 2024



Copyright: © 2024 by the authors. Licensee MDPI, Basel, Switzerland. This article is an open access article distributed under the terms and conditions of the Creative Commons Attribution (CC BY) license (<https://creativecommons.org/licenses/by/4.0/>).

Abstract: The emerging pollutant octocrylene is not efficiently removed from effluents by conventional treatment and is recurrently found in rivers. This study evaluated the adsorption of octocrylene using commercial carbon and biochar from spent coffee grounds activated with ZnCl₂. The two adsorbents had an efficiency of approximately 100% in pollutant removal throughout the experimental design. The kinetics and equilibrium isotherms showed a good correlation with the experimental data. The kinetics showed adsorption of the contaminant in 40 min for both adsorbents. The model equilibrium isotherms with the best fit and adsorption capacity was Langmuir for biochar, with a capacity of $37.822 \pm 0.005 \mu\text{g}\cdot\text{mg}^{-1}$ compared to $33.602 \pm 0.202 \mu\text{g}\cdot\text{mg}^{-1}$ for commercial carbon. Furthermore, a toxicity analysis of a $600 \mu\text{g}\cdot\text{L}^{-1}$ octocrylene solution was carried out before and after adsorption with the two charcoals separately, using *Allium cepa* roots. Before adsorption, the solution was phytotoxic and cytogenotoxic. After adsorption, the solution obtained for each charcoal no longer caused toxicity to the roots. The charcoals tested had high removal efficiency and adsorption capacity, a condition reiterated by the toxicity results. However, biochar better represented the Langmuir model in the adsorption process when removing octocrylene from the aqueous medium.

Keywords: sunscreen; adsorption kinetics and isotherms; removal; coffee grounds byproduct; absence of toxicity

1. Introduction

Octocrylene is the most used sunscreen worldwide in cosmetics and pharmaceutical products due to its high efficiency in protecting against ultraviolet rays and because it is a stabilizer of other solar filters, such as benzophenone-3, methoxydibenzoylmethane, and avobenzone [1,2]. This filter is a cinnamate ester, with a molecular weight of $361.49 \text{ g}\cdot\text{mol}^{-1}$, octanol–water partition coefficient of 6.88, low solubility in water, high resistance to photodegradation, and high lipophilicity [3,4].

Octocrylene is classified as an emerging pollutant because it is not included in environmental regulations [4,5]. Conventional treatments are not efficient in completely removing it from wastewater [4,6] and it is commonly found in surface waters on the

microgram (μg) scale [7,8]. In sewage treatment plants in different countries, raw and treated effluents presented octocrylene in concentrations ranging from micrograms to nanograms [4,5]. This compound has a high bioaccumulation potential and is persistent in freshwater resources [4].

Environmental impact assessment studies on aquatic species showed that octocrylene at environmentally relevant concentrations inhibited growth and caused mortality in microcrustaceans [9]. Furthermore, it triggered cellular toxicity and oxidative stress in mollusks [10], physiological changes in corals [11], and toxicity and endocrine disorders in fish [12,13]. Organisms (plants and earthworms) exposed to this filter, mainly by incorporating biosolids in agricultural areas and by leaching from contaminated soils, suffered from high systemic and cellular toxicity [4,5]. In addition to environmental issues, the contamination of surface waters with this compound directly impacts human populations since this sunscreen is found in drinking water on the nanogram (ng) scale [4,5]. Therefore, alternative, low-cost methods to complement conventional treatment for efficiently removing octocrylene from wastewater must be evaluated.

There are few studies in the literature evaluating non-conventional techniques for removing octocrylene from the aqueous medium. The non-usual methods, including membrane bioreactors and fungal bioremediation, proved not entirely promising due to the high lipophilic nature of this compound and the high cost of implementing the techniques [14].

Among the alternative methods to conventional treatment is adsorption on activated carbon, considered a low-cost process compared to other techniques, such as ionic liquid and ultraviolet rays, as it does not require pre-treatment and can reuse waste considered recalcitrant in the environment, such as spent coffee grounds [15]. Activations cause modifications on the charcoal surface and quantify different surface functional groups such as carboxyl, carbonyl, phenols, quinones, and lactones, facilitating the removal of pollutants in aqueous solutions [16]. After a careful search in the literature, no adsorption studies were found for octocrylene sunscreen.

Activated carbons are used to treat industrial waste and water supplies. Their application occurs due to their high capacity to interact with organic pollutants in aqueous and gaseous media. Activated carbons are classified as granules, powders, and pellets according to their size and defined [17], micro, meso, and macropores, correlated to their physical form of activation, chemical, and biological [16]. The activated carbon surface can accommodate elements such as oxygen, hydrogen, and nitrogen in the form of functional groups arising from the physical, chemical, or biological activation process. For the most part, the solid interface is predominantly composed of oxygenated functional groups, such as carboxylic acids, hydroxyl groups (when associated with aromatic chains, they confer a phenolic character), carbonyls, lactones, and quinones [18,19].

Consumption of coffee (*Coffea arabica* L.) globally exceeds nine billion kilos per year. On average, one kilogram of soluble coffee produces two kilograms of wet coffee grounds [20]. Much of this material is sent to landfills, becoming an environmental problem due to its persistence in the soil and water [20,21]. Studies have shown that biochar from spent coffee grounds is highly efficient in removing metals, textile and food dyes, and herbicides [15,22].

Biochar is a functional material developed from natural or industrial by-products, such as sludge and forestry waste. Its applicability focuses on removing aquatic pollutants [23]. Its production process is similar to charcoal activation. However, biochar needs to change its physical properties so that its adsorption capacity is similar to or greater than activated carbon [24]. The advantage of using biochar is that using by-products can make a viable economy, reduce the greenhouse effect and global warming, and increase harvest yield and productivity [24].

Biochar from spent coffee grounds is of great interest because (*Coffea arabica*) is the second most traded product in the world, and Brazil is the largest producer of this food [25]. The residue produces around 2.1 billion per harvest of *Coffea arabica* [15]. This material has around fifty percent carbon on its surface; in the pyrolysis processes, more volatile compounds such as

oxygen and hydrogen break their bonds with the carbonic mass, detaching from the molecular structure [26,27]. This calcination process forms a porous structure of the biochar, and its adsorption capacity will depend on the physical-chemical properties of the material obtained and can be enhanced by the type of activation, chemical, physical, or biological, pyrolysis time, and temperature [26,27]. Coffee grounds found in water resources can be toxic to aquatic animals due to the high concentration of caffeine [28,29].

Therefore, considering the significant adverse effects of octocrylene on different species, the lack of studies that evaluate alternative and low-cost techniques for effectively removing this compound from wastewater, and the nonexistence of adsorption studies for this solar filter, the present study aimed to assess the efficiency of commercial carbon and biochar from spent coffee grounds in removing octocrylene from the aqueous medium. This manuscript brings important results due to: evaluating, for the first time, adsorption techniques using charcoal (commercial and biochar) to remove octacrylene solar filter from the aqueous medium; and using, for the first time, biochar from used coffee grounds (a recalcitrant residue in soil and water, produced on a large scale around the world) to remove octacrylene from the aqueous medium.

2. Material and Methods

2.1. Obtaining Octocrylene

Octocrylene (2-ethylhexyl-2-cyano-3,3-diphenyl-2-propenoate, CAS 6197-30-4) was obtained from Sigma-Aldrich, (San Louis, MI, USA) in analytical grade, i.e., 100% purity, as were the other reagents used in this study.

Methodology of Adsorption

2.2. Efficiency Removal

Adsorption tests were carried out on commercial carbon purchased from Exôdus (Brazil) and charcoal (biochar) activated with ZnCl_2 . Commercial coal has only carbon and hydrogen as its structure, has a BET surface area of $543.4 \text{ m}^2 \cdot \text{g}^{-1}$ and particle sizes between 1.4 and 2 mm [30]. Biochar was produced from coffee grounds, a predominating carbon and lignocellulosic material. In the Rocha study [15], the surface area was $564.4 \text{ m}^2 \cdot \text{g}^{-1}$, pore volume was $0.32 \text{ cm}^3 \cdot \text{g}^{-1}$, and micropore volume was $0.25 \text{ cm}^3 \cdot \text{g}^{-1}$. It was carried out using ZnCl_2 in a 2:1 ratio (spent coffee grounds: chemical reagent) at 85°C for 7 h, after which the temperature was increased to 110°C for 24 h. After cooling the material and stabilizing the moisture, the sample was calcined in a muffle furnace Coel (Manaus, Brazil) at 600°C for two hours in an inert nitrogen atmosphere, with a flow rate of approximately $1 \text{ mL} \cdot \text{min}^{-1}$ of gas. Finally, activated charcoal was obtained by washing it with 0.1 M HCl for 20 min and subsequently with deionized water at 85°C for 20 min at 25°C on 100 mesh sieves to standardize the charcoal size. The spent coffee grounds were provided by the COAMO company (Campo Mourão, Brazil).

The study started with the optimization of the octocrylene concentration and amount of adsorbent, as listed in Table 1. For all runs (Table 1), after the adsorbent material produced was standardized on a 10 mesh sieve, physical variables were controlled, such as controlled temperature and agitation speed, equipment was calibrated without octocrylene, and such procedures were carried out so as not to affect the parameters of the adsorption process [31,32]. The pollutant removal efficiency tests were carried out in triplicate in order to minimize all random errors involved in the experiment.

A 2^2 factorial design duplicate at the central points was carried out to investigate two variables at two levels. The factors were defined as lower (−1), upper (1), central point (0), and extreme points (−1.41, 1.41) to adjust the Montgomery curvature [33]. The variables analyzed were adsorbent mass quantity (x_1) and octocrylene concentration (x_2). The adsorbent ranged from 5 to 15 g, and the pollutant ranged from 200 to $600 \mu\text{g} \cdot \text{L}^{-1}$.

Table 1. Experimental design of the pollutant octocrylene.

Run (R)	Adsorbent Mass (mg) x_1	Octocrylene Concentration ($\mu\text{g}\cdot\text{L}^{-1}$) x_2	ER (%)	
			Commercial Carbon	Biochar
R1	5 (−1)	200 (−1)	90.2 ± 0.1	95.1 ± 0.3
R2	5 (−1)	600 (1)	98.2 ± 0.1	99.2 ± 0.1
R3	15 (1)	200 (−1)	92.4 ± 0.3	93.0 ± 0.4
R4	15 (1)	600 (1)	95.3 ± 0.2	95.9 ± 0.2
R5	2.9 (−1.41)	400 (0)	90.8 ± 1.8	89.5 ± 0.5
R6	17.1 (1.41)	400 (0)	91.5 ± 1.5	91.0 ± 0.6
R7	10(0)	117.2 (−1.41)	93.2 ± 0.7	94.6 ± 0.1
R8	10(0)	682.8 (1.41)	98.5 ± 1.8	99.1 ± 0.1
R9	10(0)	400 (0)	98.5 ± 0.1	98.4 ± 0.1
R10	10(0)	400 (0)	96.4 ± 0.2	97.9 ± 0.1

The experimental design was used to optimize the response variable Removal Efficiency (ER). The polynomial equations were obtained by determining the dependence and independence of the factors. The significance level was a 5% difference between the average values of the tested parameters, according to Valarini [34]. All tests were carried out in triplicate under the same temperature, rotation, and time conditions.

The experiments occurred at pH = 7, and 50 mL of solution was prepared with octocrylene concentrations as listed in Table 1. The octocrylene solutions were all prepared in deionized water with 1% Tween 80. The masses in Table 1 were measured on an analytical balance (Mettler Toledo, Brazil). Then, the volumes and masses of adsorbents in the samples in Table 1 were placed in 125 mL Erlenmeyer flasks and subsequently taken to a shaker (Tecnal, Brazil) at 50 rpm at 25 °C for 24 h. After shaking, the samples were filtered and measured at a wavelength of 305 nm for octocrylene, according to Santo et al. [4]. Final concentration calculations were determined from the calibration curves of Santo et al. [4] for the conversion of absorbance into octocrylene concentration in the solution. ER(%) was determined using Equation (1).

$$ER (\%) = \left(1 - \frac{C_{Final}}{C_{initial}} \right) \times 100 \quad (1)$$

2.3. Adsorption Kinetics

Kinetic tests were performed using the best ER(%) condition. The bottles were placed under agitation in the shaker under the same conditions set in the previous item. At predetermined times, between 15 min and 1440 min, aliquots were taken, filtered, and read on a UV-VIS spectrophotometer Global Analyzer (Jaboticabal, Brazil). The experimental adsorption capacity at equilibrium (Q_e) ($\mu\text{g}\cdot\text{mg}^{-1}$) was calculated from Equation (2); where C_0 ($\mu\text{g}\cdot\text{L}^{-1}$) is the initial octocrylene concentration, C_e ($\mu\text{g}\cdot\text{L}^{-1}$) is the adsorbate concentration at equilibrium, V (L) is the solution volume, in liters, and m (mg) is the adsorbent mass, in milligrams.

$$Q_e = \frac{(C_0 - C_e) \times V}{m} \quad (2)$$

The octocrylene adsorption kinetic experimental data were fitted to pseudo-first-order (Equation (3)), and pseudo-second-order (Equation (4)) adsorption kinetic models of liquid-solid systems [35,36].

$$\frac{dQ}{dt} = k_1 \times (Q_e - Q_t) \quad (3)$$

$$\frac{dQ}{dt} = k_1 \times (Q_e - Q_t)^2 \quad (4)$$

where Q_t ($\mu\text{g}\cdot\text{mg}^{-1}$) is the total amount of emerging pollutant adsorbed in a given time, k_1 (min^{-1}) is the kinetic constant of the first order model, and k_2 ($\mu\text{g}\cdot\text{mg}^{-1}\cdot\text{min}^{-1}$) is the kinetic constant of the second-order model.

2.4. Adsorption Isotherms

The adsorption isotherms were developed using the same parameters as the previous item. The experimental points were obtained by diluting octocrylene at concentrations of 200; 400; 1000; 1300; 1600; and 2000 $\mu\text{g}\cdot\text{L}^{-1}$ in solutions of deionized water with 1% Tween 80. The experimental points were determined by Equation (2), and the liquid-solid isotherm model used in this study were the Langmuir model, Equation (5).

$$Q_e = \frac{Q_{\max} \cdot K \times C_e}{1 + K \times C_e} \quad (5)$$

where Q_{\max} ($\mu\text{g}\cdot\text{mg}^{-1}$) represents the adsorption capacity of the adsorbent at a given equilibrium concentration, and K ($\text{L}\cdot\mu\text{g}^{-1}$) refers to the affinity between the adsorbate and the adsorbent. The Langmuir isotherm describes the adsorbed phenomena on energetically homogeneous surfaces [37] and the Freundlich isotherm describes the isotherms on heterogeneous surfaces (Equation (6)).

$$Q_e = K_F \times C^{1/n} \quad (6)$$

where K_F ($\mu\text{g}\cdot\text{mg}^{-1}\cdot\text{L}^{-1}$) is defined as the adsorption intensity, and n is related to the energetic surface of the adsorption. The Freundlich model refers to the adsorption of adsorbate on heterogeneous surfaces.

2.5. Assessment of the Phytotoxic, Cytotoxic, and Genotoxic Potential of Octocrylene in Aqueous Medium before and after Adsorption with Commercial Carbon and Activated Biochar, on *Allium cepa* L. (onion) Roots

Toxicity tests on *A. cepa* roots were carried out to evaluate the efficiency of commercial carbon and biochar from spent coffee grounds in removing octocrylene from the aqueous medium.

For the tests, a concentration of 600 $\mu\text{g}\cdot\text{L}^{-1}$ of octocrylene was evaluated. This concentration was prepared in a solution of deionized water with 1% Tween 80. This concentration was chosen because, in wastewater from different locations around the world, octocrylene was found in concentrations ranging from 50 to 600 $\mu\text{g}\cdot\text{L}^{-1}$, according to Santo et al. [4] and Nascimento et al. [5].

A. cepa bulbs free from pesticides and synthetic fertilizers were obtained from an organic garden. After removing the dry cataphylls, the bulbs were washed in deionized water. Then, onions were placed in contact with the sunscreen solution at a concentration of 600 $\mu\text{g}\cdot\text{L}^{-1}$, with the solution after adsorption on commercial carbon, with the solution after adsorption on biochar, and with distilled water (used as control), and placed in a BOD incubator Cinelab (Campinas, Brazil) for 120 h, without the presence of light, for rooting. The control and analyzed solutions were called treatments. For the analysis of each treatment, five repetitions of onion bulbs were used.

Phytotoxicity, cytotoxicity, and genotoxicity tests on *A. cepa* roots were carried out according to Fiskejö [38].

To assess the phytotoxicity, the length of ten roots from each bulb repetition was measured using a manual caliper. The average root length (CMR) was determined for each treatment (Equation (7)).

$$\text{CMR}(\text{cm}) = \frac{\text{Sum of root length of root bundles}}{5} \times 100 \quad (7)$$

For cytotoxicity and genotoxicity assessments, root meristems were used. For this, on average, three roots from each bulb were collected and placed in Carnoy fixative for

24 h. Then, roots were washed in distilled water, hydrolyzed in 1 N HCl for 8 min, and washed again. Afterward, the meristematic regions of the roots were detached and crushed using a scalpel on glass slides, stained with 2% acetic orcein, and covered with a coverslip. The slides were analyzed under an optical microscope Nikon (Tokyo, Japan) using a 40× objective lens.

Cytotoxicity was determined by calculating the mitotic index (MI%), according to Equation (8), in which 2 thousand cells from each bulb were analyzed, totaling 10 thousand analyzed per treatment.

$$MI = \frac{\text{Total number of dividing cells}}{\text{Total number of cells analyzed}} \times 100 \quad (8)$$

Genotoxicity was determined by the percentage of cellular changes (CAI). From each bulb, 200 cells were analyzed, totaling 2 thousand analyzed for each treatment, according to Equation (9). The alterations considered were micronucleus, chromosome bridges, and chromosomal disorders.

$$CAI = \frac{\text{Number of cellular alterations}}{\text{Total number of cells analysed}} \times 100 \quad (9)$$

Toxicity results for the different treatments were evaluated by Kruskal–Wallis analysis of variance, followed by Dunn’s test ($p \leq 0.05$).

3. Results and Discuss

3.1. Adsorption

The experimental design required 10 experiments with octocrylene. The design adopted was the second-order model for curvature adjustment, as it is generally necessary to adjust the planning response, being the most appropriate in most cases [33]. In water treatment processes, the parameters that can affect adsorption properties must be identified.

The 2² factorial design (Table 1) used in this study aimed to obtain the best ER condition (%). The response surface methodology (RSM) was used to transform the variables into factors and optimize the laboratory experiments as the response variable ER(%) [33,34].

The results in Table 1 show the importance of optimizing experiments and reaffirm the statistical importance of conducting laboratory experiments. This process of transforming variables into factors is important when working with RSM [34]. The p -value coefficients are listed in Table 2 and have a significant effect of 0.05 in the predictive model.

Table 2. Significance test, standard error, and the respective confidence interval of the octocrylene ER(%). Combined regression variables were analyzed for adsorbent mass (mg)— x_1 and Contaminated Pollutant ($\mu\text{g}\cdot\text{L}^{-1}$)— x_2 , respectively.

Variable	Commercial Carbon				Biochar			
	ER(%)	p -Value	Standard-Error	Confidence Interval	ER(%)	p -Value	Standard-Error	Confidence Interval
A	97.48	0.000	0.735	95.4–99.5	98.16	0.000	1.469	94.823–100.0
x_1	0.11	0.890	0.367	−0.965–1.073	−0.81	0.608	0.160	−2.442–1.628
x_2	4.55	0.003	0.367	1.253–3.295	−3.35	0.084	0.734	−0.363–3.716
x_1x_2	2.62	0.065	0.520	−2.574–0.134	−0.60	0.787	1.039	−3.184–2.588
x_1^2	−6.02	0.003	0.483	−4.351–(−1.665)	−6.75	0.025	0.965	−6.054–(−0.691)
x_2^2	−1.34	0.234	0.487	−2.024–0.681	−0.20	0.992	0.972	−2.802–2.599

Table 1 lists that the removal percentage achieved in the experiment with octocrylene was more efficient with commercial carbon and biochar for run R2, in which for the octocrylene/commercial carbon system, removal was $98.2 \pm 0.1\%$ and for octocrylene/biochar

system, was $99.2 \pm 0.1\%$. In all configurations of this run, both adsorbents obtained a high ER(%), with no significant percentage differences.

Table 2 shows the p -value with a significance effect of 0.05 in the predictive model. The estimated p -value for octocrylene shows that for commercial carbon, the quadratic concentration of the pollutant (x_2), the linear amount of adsorbent (x_1), and its midpoint ($97.48 \pm 0.2\%$) are significant for the design. Thus, both factors affected the ER(%) of the pollutant. For biochar, only the midpoint and the quadratic concentration of the pollutant (x_2) interfered with the increase in pollutant removal. Therefore, for commercial carbon, both octocrylene concentration and charcoal mass can affect the removal efficiency. As for biochar interacting with octocrylene, only the pollutant concentration can affect the removal efficiency of the sunscreen. The experimental responses encoded by the factors x_1 and x_2 can also be represented by general mathematical solutions that locate the stationary point, such as Equations (10) and (11) for the octocrylene pollutant.

$$ER(\%)_{\text{Commercial Carbon}} = 97.48 + 4.55x_2 - 6.02x_1^2 \quad (10)$$

$$ER(\%)_{\text{Biochar}} = 98.16 - 6.75x_1^2 \quad (11)$$

Equations (10) and (11) show the adsorption technique with two types of charcoal tested, offering a unique analysis of each equation associated with its respective graph. Equation (10) shows that the midpoint of $ER(\%)_{\text{commercial carbon}}$ was 97.48%. In this equation, increasing the pollutant concentration and decreasing the amount of adsorbent increases the $ER(\%)_{\text{commercial carbon}}$. In Equation (11), only the amount of biochar changes the $ER(\%)_{\text{Biochar}}$, following the same trend as commercial coal, in which the smaller amount of charcoal increases the $ER(\%)_{\text{Biochar}}$. The equation models follow the same trend. This implies that each pollutant/adsorbent amount system is correlated to the type of chemical compounds and type of charcoal to be used. The R2 runs were more efficient because models with high concentrations have greater adsorption in a shorter time, i.e., they quickly stabilize adsorption [39].

The location of the stationary point is of great importance to finding the best conditions for levels x_1 and x_2 and their interactions that optimize the RSM. Contour plots play an important role in response surface studies [33]. Figure 1 illustrates that the closer to the dark red region, the higher the ER(%) for the octocrylene pollutant. Correlating Figure 1 with Equations (10) and (11), the best adsorption conditions are run R2 for both types of charcoal, as there are low concentrations of adsorbent mass and high concentrations of pollutant concentration. In this way, the adsorption kinetics of these runs and the adsorption isotherm with this mass quantity of adsorbent were considered.

ER(%) obtained high values, close to 100%, as the size of the octocrylene molecule is smaller than the sizes of the micropores of biochar and activated carbon [15]. Other physicochemical factors also contribute to the increase in ER(%), such as functional groups; a higher diversity of functional groups on the charcoal surface increases ER(%), and polarity, ionic nature, and pH of the process; chemical nature similar to the solution also cause an increase in ER(%) [40,41]. The process of biochar formation occurs by pyrolysis at 600 °C, which leads to greater formation of microporous structures in the material, improving its ER(%).

The molar mass of octocrylene of $361.48 \text{ g}\cdot\text{mol}^{-1}$ and the surface area of biochar of $564,366 \text{ m}^2\cdot\text{g}^{-1}$ [15] show that a high removal percentage occurred due to the larger surface area of the functional material compared to the pollutant concentration used in the study. The interaction of ions on the surfaces of the molecule and material also facilitates the chemisorption of reducing and oxidizing agents [42]. The surface of activated carbon without a chemical activator can accommodate elements such as oxygen, hydrogen, and nitrogen in the form of functional groups arising from the activation process. For the most part, the solid interface is predominantly composed of oxygenated functional groups, such as: carboxylic acids; hydroxyl groups (when associated with aromatic chains, they confer a phenolic character); carbonyls; lactones; quinones [18,19].

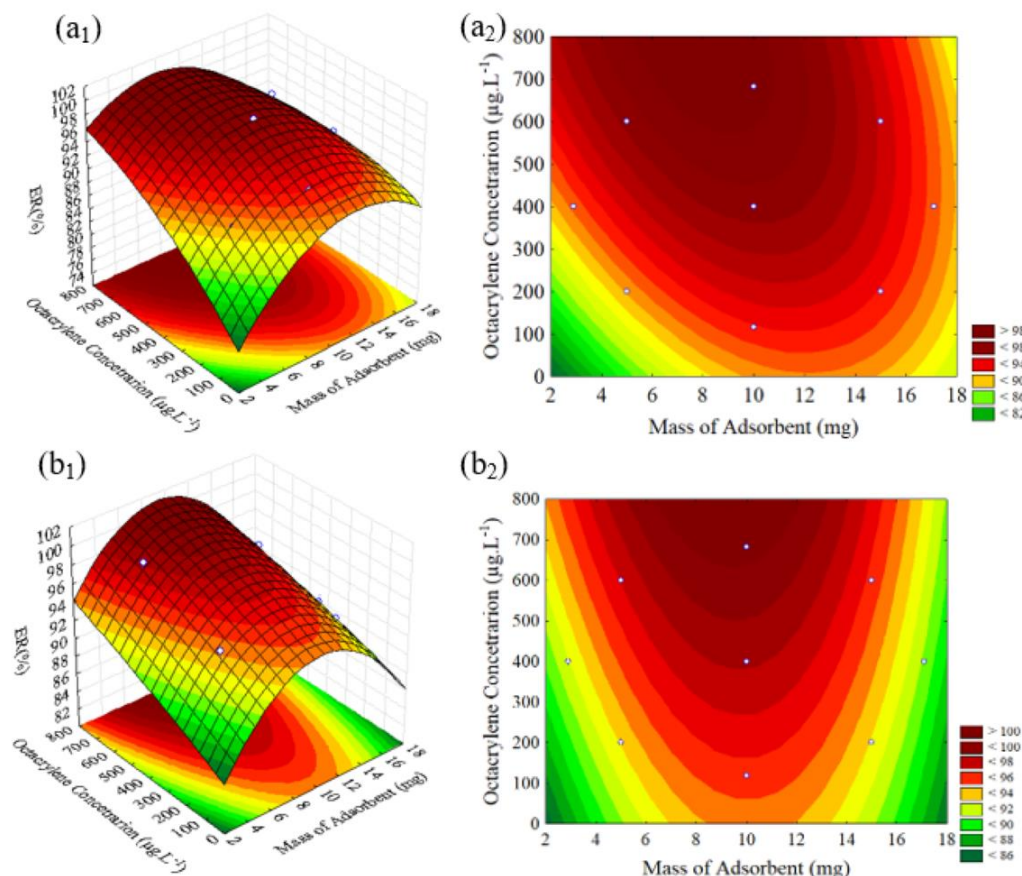


Figure 1. RSM plot of the Octacrylene Pollutant with: (a₁) RSM Commercial Carbon. (a₂) Commercial Carbon Contour Plot. (b₁) RSM Biochar. (b₂) Biochar Carbon Contour Plot.

The use of chemical activators contributes to the formation of pores and an increase in channel functional groups in the activated carbon matrix [43]. Precursor materials, such as ZnCl_2 , are used as a dehydrating effect on lignocellulosic materials, such as spent coffee grounds in natura, previously carbonized. ZnCl_2 increases the mass proportion and causes the easier release of volatile substances, so that the adsorption of nitrogen increases in the biochar, which consequently increases its surface area [44]. The use of ZnCl_2 breaks down the cellulose molecules and leads to an increase in different cavities, which causes a greater surface area on the activated carbon. Upon activation with ZnCl_2 , the yield of activated carbon increases due to polymerization by creating some aromatic compounds with large rings, facilitating the adsorption of contaminants [45].

The mechanism of interaction between octacrylene and the adsorbents biochar and commercial charcoal remains unclear. Grilla [46], Rocha [15], Mroziak [47], and Gianakopoulos [36] proposed an adsorption mechanism between the pollutant and the adsorbent that considered that the reactions occurred between radicals and non-radicals. Thus, based on assumptions, in aqueous solutions, biochar has a radical (Cl^-) and commercial charcoal only (OH^-), as it does not present any chemical agent on its surface. Next, intermediate products related to oxygen groups are generated on the surfaces of the adsorbents. The octacrylene adsorption process initially occurs on the surface of biochar and commercial charcoal due to interactions between the octacrylene aromatic ring and the functional material [48]. This occurs due to the OH^- group on the surface of the adsorbent due to the charge generated from the octacrylene in the functional material. Biochar anions can also be adsorbed on sites that contain oxygen. The OH^- groups on the surface of functional materials can participate in oxidation-reduction reactions, mainly in transferring π electrons from the adsorbed octacrylene molecule, as the aromatic phase can increase the transfer capacity of electrons displaced in the adsorption process [46].

3.2. Adsorption Kinetics

Based on the experimental design, the R2 run for commercial active carbon and biochar was used for the adsorption kinetics of octocrylene due to the higher ER (%). Figure 2 shows the trend of experimental data, determined experimentally by Equation (2). The adsorption process occurs at a concentration of $600 \mu\text{g}\cdot\text{L}^{-1}$ of octocrylene for 5 mg of adsorbent. The pseudo-first-order (Equation (3)) and pseudo-second-order (Equation (4)) kinetic models stabilize quickly, around 40 min.

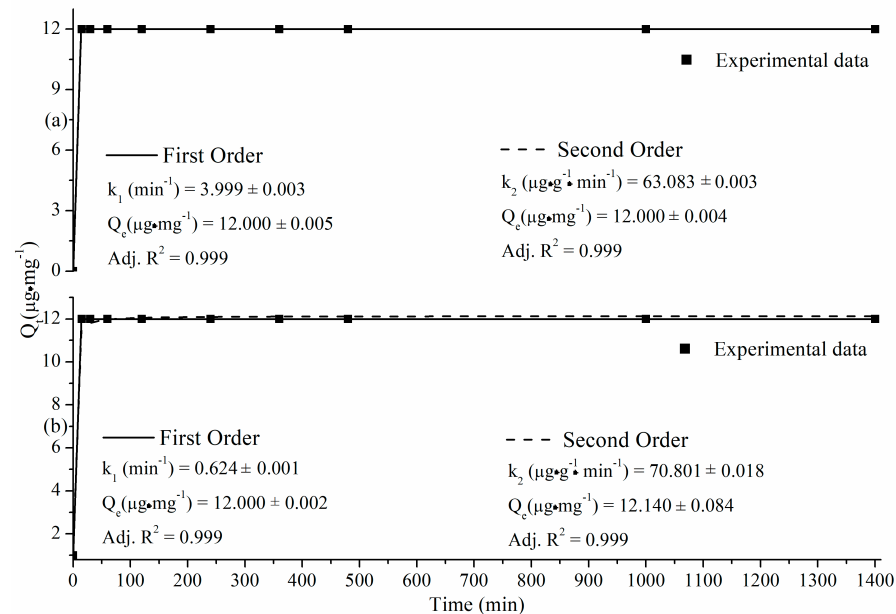


Figure 2. Adsorption kinetics and respective fits for initial concentrations of octacrylene $600 \mu\text{g}\cdot\text{L}^{-1}$ with (a) Commercial Carbon, (b) Biochar ZnCl_2 .

The rapid adsorption of octocrylene on both activated charcoals shows that the adsorption is molecular and occurs preferentially on the external surface of the adsorbent and that due to chemical activation, the active sites available in the biochar reached equilibrium quickly, to achieve the adsorption–desorption system [15,49].

Figure 2 also presents the total amount (Q_t) in $\mu\text{g}\cdot\text{L}^{-1}$ and the adsorption kinetic parameters obtained by fitting the models. From the kinetic parameters obtained under the conditions analyzed, the adjustments for both the pseudo-first-order and pseudo-second-order models represented the experimental data based on high correlation coefficient values (R^2). The tested models presented the same amount of pollutant adsorbed at equilibrium, Q_e ($\mu\text{g}\cdot\text{mg}^{-1}$), on both tested charcoals. The adsorption rate constant, k_1 (min^{-1}), for commercial carbon was higher than for biochar for pseudo-prime models. The constant intraparticle diffusion rate, k_2 ($\mu\text{g}\cdot\text{mg}^{-1}\cdot\text{min}^{-1}$), was higher for biochar than charcoal for pseudo-second-order models [50].

The two models described the experimental data with pseudo-first- and pseudo-second-order models. However, the phenomenological model to be chosen to represent the kinetic adsorption system depends on the final objective. The pseudo-first-order model is considered an excellent model for long-term adsorption processes. For this model, the most suitable polluting system is commercial carbon. The pseudo-second-order model, which also satisfactorily represented the experimental data, Adj. R^2 of 0.999, indicates that there are many complexed sites and many awaiting complexation in the activated carbon [51]; therefore, the general balance of active sites has a large number of active sites that can adsorb pollutants. Thus, the adsorption rate will depend on the amount of pollutant in the system and not on its concentration. For a low amount of pollutants, the most suitable system is biochar; otherwise, the most suitable is commercial carbon [50].

3.3. Adsorption Isotherms

The adsorption equilibrium isotherms of octocrylene using commercial carbon and biochar were analyzed here due to their importance in the interpretation of adsorption systems, whose objective is to understand the interaction of the adsorbent surface with the pollutant in a liquid medium. Therefore, the correlation between experimental data and adsorption isotherms is important for understanding adsorption systems [50]. Figure 3 presents the experimental data and the Langmuir and Freundlich models, Equations (5) and (6), respectively; for both charcoals, the tested models showed good correlation in the concentration range from $1 \times 10^{-3} \mu\text{g}\cdot\text{L}^{-1}$ to $1 \times 10^{-2} \mu\text{g}\cdot\text{L}^{-1}$ [52]. For higher concentrations, there was a tendency to stabilize the C_e and Q_e relationship in both charcoals.

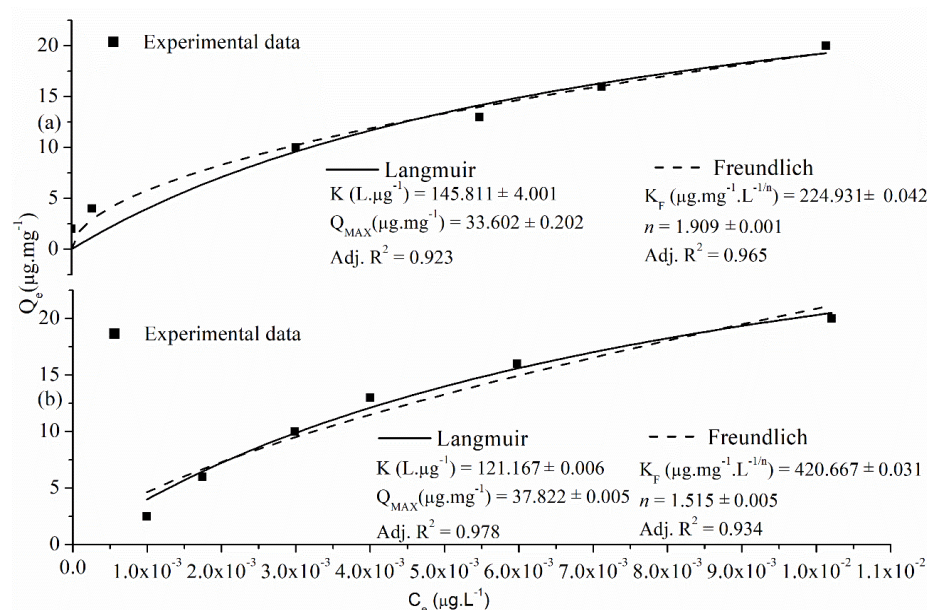


Figure 3. Octacrylene adsorption isotherms with C_0 ranging from $600 \mu\text{g}\cdot\text{L}^{-1}$: (a) Commercial Carbon, (b) Biochar ZnCl_2 .

Figure 3 also shows the kinetic parameters of the Langmuir and Freundlich models for the tested charcoals. The two isotherms showed good correlation; commercial carbon had a better affinity between the adsorbate and the adsorbent (K) in the Langmuir isotherm, and biochar showed better Q_{max} adsorption capacity and better correlation coefficient. For the Freundlich isotherm, biochar obtained better adsorption intensity (K_F), and commercial carbon presented a better energy surface. The isothermal model that best represented commercial carbon was Freundlich, in which the value of n greater than zero indicated that the adsorption process was spontaneous [15,50]. However, for biochar activated with ZnCl_2 , the Langmuir model best represented the adsorption systems. The Langmuir model shows higher values of Q_{max} and K than commercial carbon, which means that the biochar surface area, pore volume, particle size distribution, and multilayer development [15] are higher than those of commercial carbon. Another factor of great importance was the chemical activation with ZnCl_2 ; the use of this reagent increased the possibility of octocrylene binding with various functional groups on the biochar surface, such as phenolic compounds, according to Karapinar [53]. The Langmuir model presupposes adsorption processes at atmospheric pressure, homogeneous systems, monolayer and multilayer adsorption, and constant adsorption temperature, and that the process stabilizes from the saturation of active sites on the surface of functional material [54].

Considering such findings, both charcoals showed a good correlation with the pollutant; however, both commercial carbon and biochar obtained satisfactory results in $\text{ER}(\%)$, kinetics, and adsorption isotherm. Biochar becomes interesting due to the environmental and economic importance of reusing spent coffee grounds, as the insertion of biochar in

adsorption processes can minimize the environmental impact caused by this residue on freshwater water resources.

Therefore, the ideal model and system for large-scale application is the Langmuir model and the functional model, because this model adequately represents homogeneous monolayer surfaces and has environmental and economic appeal [54]. This charcoal has an advantageous use because spent coffee grounds are not reused in the economic environment to date, and as previously mentioned, if improperly discarded, they can be toxic to aquatic and terrestrial organisms due to constituents such as caffeine, fatty acids, and metals [55].

3.4. Toxic Potential

Worldwide, for more than five decades, *A. cepa* roots have been used to evaluate the ecotoxicity (phytotoxicity, cytotoxicity, and genotoxicity) of natural and wastewater, and environmental pollutants, even when their concentrations in the medium are on the scale of nanograms, proving highly sensitive to xenobiotics [5,56,57]. The results obtained with this biological system show a high correlation with the results obtained in other bioassays, such as in different plants, animals, and cell cultures [5,56–58].

In Table 3, the octocrylene solution at a concentration of $600 \mu\text{g}\cdot\text{L}^{-1}$, before adsorption caused a significant reduction in root elongation compared to the control results. Furthermore, it caused disturbances in cell division in the meristems, with a mitotic index of less than 60%. In addition to mitosis disorders, as shown in Table 4, octocrylene also induced the development of cellular alterations in significant numbers in meristematic cells. Therefore, under the established analysis conditions, octocrylene was phytotoxic, cytotoxic, and genotoxic to onion roots.

Table 3. Average growth and mitotic index of *Allium cepa* L. roots exposed to octocrylene solution at $600 \mu\text{g}\cdot\text{L}^{-1}$, before and after adsorption on commercial carbon or charcoal from spent coffee grounds, for 120 h.

TR	ARL/SD	MI/SD (%)
Co	100 ± 1.0	100 ± 0.9
OCS before adsorption	51.9 ± 1.1	52.7 ± 0.9
OCS after adsorption on commercial carbon	89.1 ± 1.1	85.5 ± 1.3
OCS after adsorption on biochar	$94.7 \pm 0.9^*$	$97.3 \pm 1.0^*$

OCS: octocrylene solution, TR: Treatment, ARL: average root length, MI: Mitotic Index, CAI: cellular alteration index, SD: Standard Deviation, Co: Control. For ARL and MI, data are expressed as a percentage of control values. * Significantly different from the Co, according to Kruskal–Wallis H followed by Dunn’s posthoc test ($p \leq 0.05$).

Table 4. Number, types, and cellular alteration index in *A. cepa* bulb root meristem cells exposed to octocrylene solution at $600 \mu\text{g}\cdot\text{L}^{-1}$, before and after adsorption on commercial carbon or charcoal from spent coffee grounds, for 120 h.

TR	Number and Type of Cellular Changes			
	Micronucleus	Chromosome Bridges	Chromosomal Derangements	CAI \pm SD (%)
Co	3	0	0	0.15
OCS before adsorption	87	42	72	10.1
OCS after adsorption on commercial carbon	1	6	0	0.35
OCS after adsorption on biochar	2	1	0	0.15

OCS: octocrylene solution, TR: Treatment, Conc.: Concentration, Co: Control (distilled water), CAI: Cellular Alteration Index; SD: Standard Deviation.

The results in Tables 3 and 4 with the octocrylene solution before adsorption corroborate the results of Santos [4] and Nascimento [5], who evaluated this sunscreen at concentrations of 10, 100, and 1000 $\mu\text{g}\cdot\text{L}^{-1}$, in cultivated (*Allium cepa* L., *Lactuca sativa* L., *Cucumis sativus* L., *Lycopersicum esculentum* Mill., and *Daucus carota* L.) and uncultivated (*Avena fatua* L. and *Taraxacum officinale*) species and reported high toxicity and oxidative stress caused by these compounds to plants.

Roots exposed to octocrylene solutions obtained after adsorption on commercial carbon and after adsorption on biochar had no reduction in root length, nor did they reduce the cell division rate or cause significant cellular changes when compared to the control, proving non-phytotoxic, non-cytotoxic, and non-genotoxic (Tables 3 and 4).

4. Conclusions

This study investigated the efficiency of removing the pollutant octocrylene using commercial carbon and biochar activated with ZnCl_2 . From the results obtained, ZnCl_2 -based charcoal obtained better results than commercial carbon due to all the factors involved, such as the reuse of a persistent product in the environment and high removal efficiency for high concentrations of octocrylene in an aqueous solution.

First- and second-order kinetics were simulated in this study, showing that adsorption reaches adsorption/desorption equilibrium at around 40 min, with a similar Q_e ($\mu\text{g}\cdot\text{mg}^{-1}$) for the first- and second-order models. The tested adsorption isotherms, Langmuir and Freundlich, had excellent correlations with the tested experimental data. The model that best suited the experimental data were Langmuir.

Finally, the ecotoxicity results obtained by the *A. cepa* bioassay prove the effectiveness of the adsorbents tested to remove octocrylene from the aqueous medium and show that after adsorption on commercial carbon and biochar, the solution obtained is no longer toxic.

Author Contributions: Conceptualization, A.P.P. and O.V.J.; methodology, S.A.F.d.R., B.C.d.S.R., L.E.Z.d.M., J.M.P.V., D.S., D.E.S. and R.d.S.G.; writing—original draft preparation, A.P.P.; writing—review and editing, A.P.P. and O.V.J. All authors have read and agreed to the published version of the manuscript.

Funding: This research received no external funding.

Data Availability Statement: We declare that all data are in the manuscript. Therefore, the Data availability statement does not apply to this study.

Acknowledgments: The authors would like to thank the Multi-User Laboratory at the Londrina Campus, the Multi-User Research Support Laboratory at the Apucarana Campus, the Multi-User Analytical Center and the Multi-User Materials Characterization Center at the Campo Mourão Campus, at the Federal Technological University of Paraná, for supporting the measurements.

Conflicts of Interest: The authors declare no conflicts of interests.

References

1. Duis, K.; Junker, T.; Coors, A. Review of the Environmental Fate and Effects of Two UV Filter Substances Used in Cosmetic Products. *Sci. Total Environ.* **2022**, *808*, 151931. [[CrossRef](#)] [[PubMed](#)]
2. Zhong, X.; Downs, C.A.; Li, Y.; Zhang, Z.; Li, Y.; Liu, B.; Gao, H.; Li, Q. Comparison of Toxicological Effects of Oxybenzone, Avobenzone, Octocrylene, and Octinoxate Sunscreen Ingredients on Cucumber Plants (*Cucumis sativus* L.). *Sci. Total Environ.* **2020**, *714*, 136879. [[CrossRef](#)]
3. Pawlowski, S.; Lanzinger, A.C.; Dolich, T.; Füßl, S.; Salinas, E.R.; Zok, S.; Weiss, B.; Hefner, N.; Van Sloun, P.; Hombeck, H.; et al. Evaluation of the Bioaccumulation of Octocrylene after Dietary and Aqueous Exposure. *Sci. Total Environ.* **2019**, *672*, 669–679. [[CrossRef](#)] [[PubMed](#)]
4. Santo, D.E.; Dusman, E.; da Silva Gonzalez, R.; Romero, A.L.; dos Santos Gonçalves do Nascimento, G.C.; de Souza Moura, M.A.; Bressiani, P.A.; Filipi, Á.C.K.; Gomes, E.M.V.; Pokrywiecki, J.C.; et al. Prospecting Toxicity of Octocrylene in *Allium cepa* L. and *Eisenia fetida* Sav. *Environ. Sci. Pollut. Res.* **2023**, *30*, 8257–8268. [[CrossRef](#)] [[PubMed](#)]

5. dos Santos Gonçalves Nascimento, G.C.; da Cunha Barros, D.G.; Ratuchinski, L.S.; Okon, C.; Bressiani, P.A.; Santo, D.E.; Duarte, C.C.S.; Ferreira, P.M.P.; Junior, O.V.; Pokrywiecki, J.C.; et al. Adverse Effects of Octocrylene on Cultivated and Spontaneous Plants and in Soil Animal. *Water. Air. Soil Pollut.* **2023**, *234*, 757. [\[CrossRef\]](#)
6. Trebše, P.; Polyakova, O.V.; Baranova, M.; Kralj, M.B.; Dolenc, D.; Sarakha, M.; Kutin, A.; Lebedev, A.T. Transformation of Avobenzone in Conditions of Aquatic Chlorination and UV-Irradiation. *Water Res.* **2016**, *101*, 95–102. [\[CrossRef\]](#)
7. Hopkins, Z.R.; Snowberger, S.; Blaney, L. Ozonation of the Oxybenzone, Octinoxate, and Octocrylene UV-Filters: Reaction Kinetics, Absorbance Characteristics, and Transformation Products. *J. Hazard. Mater.* **2017**, *338*, 23–32. [\[CrossRef\]](#)
8. Labille, J.; Slomberg, D.; Catalano, R.; Robert, S.; Apers-Tremelo, M.L.; Boudenne, J.L.; Manasfi, T.; Radakovitch, O. Assessing UV Filter Inputs into Beach Waters during Recreational Activity: A Field Study of Three French Mediterranean Beaches from Consumer Survey to Water Analysis. *Sci. Total Environ.* **2020**, *706*, 136010. [\[CrossRef\]](#)
9. Boyd, A.; Stewart, C.B.; Philibert, D.A.; How, Z.T.; El-Din, M.G.; Tierney, K.B.; Blewett, T.A. A Burning Issue: The Effect of Organic Ultraviolet Filter Exposure on the Behaviour and Physiology of *Daphnia magna*. *Sci. Total Environ.* **2021**, *750*, 141707. [\[CrossRef\]](#)
10. Giraldo, A.; Montes, R.; Rodil, R.; Quintana, J.B.; Vidal-Liñán, L.; Beiras, R. Ecotoxicological Evaluation of the UV Filters Ethylhexyl Dimethyl P-Aminobenzoic Acid and Octocrylene Using Marine Organisms *Isochrysis galbana*, *Mytilus galloprovincialis* and *Paracentrotus lividus*. *Arch. Environ. Contam. Toxicol.* **2017**, *72*, 606–611. [\[CrossRef\]](#)
11. Stien, D.; Clergeaud, F.; Rodrigues, A.M.S.; Lebaron, K.; Pillot, R.; Romans, P.; Fagervold, S.; Lebaron, P. Metabolomics Reveal That Octocrylene Accumulates in *Pocillopora damicornis* Tissues as Fatty Acid Conjugates and Triggers Coral Cell Mitochondrial Dysfunction. *Anal. Chem.* **2019**, *91*, 990–995. [\[CrossRef\]](#) [\[PubMed\]](#)
12. Yan, S.; Liang, M.; Chen, R.; Hong, X.; Zha, J. Reproductive Toxicity and Estrogen Activity in Japanese Medaka (*Oryzias latipes*) Exposed to Environmentally Relevant Concentrations of Octocrylene. *Environ. Pollut.* **2020**, *261*, 114104. [\[CrossRef\]](#) [\[PubMed\]](#)
13. Meng, Q.; Yeung, K.; Chan, K.M. Toxic Effects of Octocrylene on Zebrafish Larvae and Liver Cell Line (ZFL). *Aquat. Toxicol.* **2021**, *236*, 105843. [\[CrossRef\]](#) [\[PubMed\]](#)
14. Tran, H.T.; Dang, B.T.; Thuy, L.T.T.; Hoang, H.G.; Bui, X.T.; Le, V.G.; Lin, C.; Nguyen, M.K.; Nguyen, K.Q.; Nguyen, P.T.; et al. Advanced Treatment Technologies for the Removal of Organic Chemical Sunscreens from Wastewater: A Review. *Curr. Pollut. Rep.* **2022**, *8*, 288–302. [\[CrossRef\]](#)
15. Rocha, B.C.d.S.; de Moraes, L.E.Z.; Santo, D.E.; Peron, A.P.; de Souza, D.C.; Bona, E.; Valarini, O. Removal of Bentazone Using Activated Carbon from Spent Coffee Grounds. *J. Chem. Technol. Biotechnol.* **2024**, *99*, 1342–1355. [\[CrossRef\]](#)
16. Sultana, M.; Rownok, M.H.; Sabrin, M.; Rahaman, M.H.; Alam, S.M.N. A Review on Experimental Chemically Modified Activated Carbon to Enhance Dye and Heavy Metals Adsorption. *Clean. Eng. Technol.* **2022**, *6*, 100382. [\[CrossRef\]](#)
17. Wang, H.; Zhang, Z.; Sun, R.; Lin, H.; Gong, L.; Fang, M.; Hu, W.H. HPV Infection and Anemia Status Stratify the Survival of Early T2 Laryngeal Squamous Cell Carcinoma. *J. Voice* **2015**, *29*, 356–362. [\[CrossRef\]](#) [\[PubMed\]](#)
18. Boehm, H.P. Surface Oxides on Carbon and Their Analysis: A Critical Assessment. *Carbon* **2002**, *40*, 145–149. [\[CrossRef\]](#)
19. Boehm, H.P. Some Aspects of the Surface Chemistry of Carbon Blacks and Other Carbons. *Carbon* **1994**, *32*, 759–769. [\[CrossRef\]](#)
20. Bagiu, I.C.; Sarac, I.; Radu, F.; Bostan, C.; Butnariu, M.; Bagiu, R.V. Ecotechnologies for Persistent Pollutants. In *Bioremediation and Biotechnology*; Springer: Berlin/Heidelberg, Germany, 2020; Volume 3, pp. 105–138. [\[CrossRef\]](#)
21. Ijanu, E.M.; Kamaruddin, M.A.; Norashiddin, F.A. Coffee Processing Wastewater Treatment: A Critical Review on Current Treatment Technologies with a Proposed Alternative. *Appl. Water Sci.* **2020**, *10*, 11. [\[CrossRef\]](#)
22. Chen, S.S.; Yu, I.K.M.; Cho, D.W.; Song, H.; Tsang, D.C.W.; Tessonnier, J.P.; Ok, Y.S.; Poon, C.S. Selective Glucose Isomerization to Fructose via a Nitrogen-Doped Solid Base Catalyst Derived from Spent Coffee Grounds. *ACS Sustain. Chem. Eng.* **2018**, *6*, 16113–16120. [\[CrossRef\]](#)
23. Jagadeesh, N.; Sundaram, B. Adsorption of Pollutants from Wastewater by Biochar: A Review. *J. Hazard. Mater. Adv.* **2023**, *9*, 100226. [\[CrossRef\]](#)
24. Cheng, N.; Wang, B.; Wu, P.; Lee, X.; Xing, Y.; Chen, M.; Gao, B. Adsorption of Emerging Contaminants from Water and Wastewater by Modified Biochar: A Review. *Environ. Pollut.* **2021**, *273*, 116448. [\[CrossRef\]](#)
25. Siregar, C.A.; Siregar, A.M.; Lubis, R.W.; Marpaung, D. Rancang Bangun Mesin Giling Kopi Untuk Menunjang Dan Membuka Unit Usaha Baru Mitra Deli Coffe. *ABDI SABHA (J. Pengabd. Kpd. Masy.)* **2022**, 174–180.
26. Javier Sánchez, A. *Characterization of Activated Carbon Produced from Coffee Residues by Chemical and Physical Activation*; KTH, School of Chemical Science and Engineering: Stockholm, Sweden, 2011; Volume 66.
27. Jagdale, P.; Ziegler, D.; Rovere, M.; Tulliani, J.M.; Tagliaferro, A. Waste Coffee Ground Biochar: A Material for Humidity Sensors. *Sensors* **2019**, *19*, 801. [\[CrossRef\]](#) [\[PubMed\]](#)
28. Fernandes, A.S.; Mello, F.V.C.; Thode Filho, S.; Carpes, R.M.; Honório, J.G.; Marques, M.R.C.; Felzenszwalb, I.; Ferraz, E.R.A. Impacts of Discarded Coffee Waste on Human and Environmental Health. *Ecotoxicol. Environ. Saf.* **2017**, *141*, 30–36. [\[CrossRef\]](#) [\[PubMed\]](#)
29. Ferraz, F.M.; Yuan, Q. Organic Matter Removal from Landfill Leachate by Adsorption Using Spent Coffee Grounds Activated Carbon. *Sustain. Mater. Technol.* **2020**, *23*, e00141. [\[CrossRef\]](#)

30. Haro, N.K.; Dávila, I.V.J.; Nunes, K.G.P.; de Franco, M.A.E.; Marcilio, N.R.; Féris, L.A. Kinetic, Equilibrium and Thermodynamic Studies of the Adsorption of Paracetamol in Activated Carbon in Batch Model and Fixed-Bed Column. *Appl. Water Sci.* **2021**, *11*, 38. [\[CrossRef\]](#)
31. Debien, I.C.N.; Vardanega, R.; Santos, D.T.; Meireles, M.A.A. Pressurized Liquid Extraction as a Promising and Economically Feasible Technique for Obtaining Beta-Ecdysone-Rich Extracts from Brazilian Ginseng (*Pfaffia glomerata*) Roots. *Sep. Sci. Technol.* **2015**, *50*, 1647–1657. [\[CrossRef\]](#)
32. Dean, J.R. Pressurized Liquid Extraction. In *Extraction Techniques for Environmental Analysis*; Wiley: Hoboken, NJ, USA, 2022; pp. 171–204. [\[CrossRef\]](#)
33. Montgomery, D.C. *Design and Analysis of Experiments*, 8th ed.; Wiley: Hoboken, NJ, USA, 2012; Volume 2, ISBN 9781118146927.
34. Valarini Junior, O.; Reitz Cardoso, F.A.; Machado Giufrida, W.; de Souza, M.F.; Cardozo-Filho, L. Production and Computational Fluid Dynamics-Based Modeling of PMMA Nanoparticles Impregnated with Ivermectin by a Supercritical Antisolvent Process. *J. CO₂ Util.* **2019**, *35*, 47–58. [\[CrossRef\]](#)
35. Gonçalves Júnior, D.R.; de Araújo, P.C.C.; Simões, A.L.G.; Voll, F.A.P.; Parizi, M.P.S.; de Oliveira, L.H.; Ferreira-Pinto, L.; Cardozo-Filho, L.; de Jesus Santos, E. Assessment of the Adsorption Capacity of Phenol on Magnetic Activated Carbon. *Asia-Pac. J. Chem. Eng.* **2022**, *17*, e2725. [\[CrossRef\]](#)
36. Tan, K.L.; Hameed, B.H. Insight into the Adsorption Kinetics Models for the Removal of Contaminants from Aqueous Solutions. *J. Taiwan Inst. Chem. Eng.* **2017**, *74*, 25–48. [\[CrossRef\]](#)
37. Karri, R.R.; Sahu, J.N.; Jayakumar, N.S. Optimal Isotherm Parameters for Phenol Adsorption from Aqueous Solutions onto Coconut Shell Based Activated Carbon: Error Analysis of Linear and Non-Linear Methods. *J. Taiwan Inst. Chem. Eng.* **2017**, *80*, 472–487. [\[CrossRef\]](#)
38. Fiskesjö, G. The Allium Test as a Standard in Environmental Monitoring. *Hereditas* **1985**, *102*, 99–112. [\[CrossRef\]](#)
39. Liu, Y.; Shen, L. From Langmuir Kinetics to First- and Second-Order Rate Equations for Adsorption. *Langmuir* **2008**, *24*, 11625–11630. [\[CrossRef\]](#)
40. Amin, F.R.; Huang, Y.; He, Y.; Zhang, R.; Liu, G.; Chen, C. Biochar Applications and Modern Techniques for Characterization. *Clean Technol. Environ. Policy* **2016**, *18*, 1457–1473. [\[CrossRef\]](#)
41. Huang, Q.; Song, S.; Chen, Z.; Hu, B.; Chen, J.; Wang, X. Biochar-Based Materials and Their Applications in Removal of Organic Contaminants from Wastewater: State-of-the-Art Review. *Biochar* **2019**, *1*, 45–73. [\[CrossRef\]](#)
42. Wang, H.; Lei, X.; Khu, S.T.; Song, L. Optimization of Pump Start-up Depth in Drainage Pumping Station Based on SWMM and PSO. *Water* **2019**, *11*, 2. [\[CrossRef\]](#)
43. Fletcher, A.; Somorin, T.; Aladeokin, O. Production of High Surface Area Activated Carbon from Peanut Shell by Chemical Activation with Zinc Chloride: Optimisation and Characterization. *Bioenergy Res.* **2024**, *17*, 467–478. [\[CrossRef\]](#)
44. Heidarinejad, Z.; Dehghani, M.H.; Heidari, M.; Javedan, G.; Ali, I.; Sillanpää, M. Methods for Preparation and Activation of Activated Carbon: A Review. *Environ. Chem. Lett.* **2020**, *18*, 393–415. [\[CrossRef\]](#)
45. Anisuzzaman, S.M.; Joseph, C.G.; Krishnaiah, D.; Bono, A.; Suali, E.; Abang, S.; Fai, L.M. Removal of Chlorinated Phenol from Aqueous Media by Guava Seed (*Psidium guajava*) Tailored Activated Carbon. *Water Resour. Ind.* **2016**, *16*, 29–36. [\[CrossRef\]](#)
46. Grilla, E.; Vakros, J.; Konstantinou, I.; Manariotis, I.D.; Mantzavinos, D. Activation of Persulfate by Biochar from Spent Malt Rootlets for the Degradation of Trimethoprim in the Presence of Inorganic Ions. *J. Chem. Technol. Biotechnol.* **2020**, *95*, 2348–2358. [\[CrossRef\]](#)
47. Mrozik, W.; Minofar, B.; Thongsamer, T.; Wiriaphong, N.; Khawkomol, S.; Plaimart, J.; Vakros, J.; Karapanagioti, H.; Vinitnantharat, S.; Werner, D. Valorisation of Agricultural Waste Derived Biochars in Aquaculture to Remove Organic Micropollutants from Water—Experimental Study and Molecular Dynamics Simulations. *J. Environ. Manag.* **2021**, *300*, 113717. [\[CrossRef\]](#) [\[PubMed\]](#)
48. Heo, J.; Yoon, Y.; Lee, G.; Kim, Y.; Han, J.; Park, C.M. Enhanced Adsorption of Bisphenol A and Sulfamethoxazole by a Novel Magnetic CuZnFe₂O₄–Biochar Composite. *Bioresour. Technol.* **2019**, *281*, 179–187. [\[CrossRef\]](#) [\[PubMed\]](#)
49. do Nascimento, R.F.; de Lima, A.C.A.; Vidal, C.B.; Melo, D.d.Q.; Raulino, G.S.C. *Adsorção: Aspectos Teóricos e Aplicações Ambientais*; Imprensa Universitária: Fortaleza, Brazil, 2020; p. 308.
50. Benaouda, B.; Iman, G.; Michalkiewicz, B. Study on Anionic Dye Toxicity Reduction from Simulated Media by MnO₂/Agro-Biomass Based-AC Composite Adsorbent. *Ind. Crops Prod.* **2024**, *208*, 117789. [\[CrossRef\]](#)
51. Wang, J.; Guo, X. Adsorption Kinetic Models: Physical Meanings, Applications, and Solving Methods. *J. Hazard. Mater.* **2020**, *390*, 122156. [\[CrossRef\]](#)
52. McCabe, W.C.; Smith, J.C.; Harriot, P. *Unit Operations of Chemical Engineering*; McGraw-Hill: New York, NY, USA, 1993; Volume 30. [\[CrossRef\]](#)
53. Karapinar, H.S. Adsorption Performance of Activated Carbon Synthesis by ZnCl₂, KOH, H₃PO₄ with Different Activation Temperatures from Mixed Fruit Seeds. *Environ. Technol.* **2022**, *43*, 1417–1435. [\[CrossRef\]](#) [\[PubMed\]](#)
54. Mozaffari Majd, M.; Kordzadeh-Kermani, V.; Ghalandari, V.; Askari, A.; Sillanpää, M. Adsorption Isotherm Models: A Comprehensive and Systematic Review (2010–2020). *Sci. Total Environ.* **2022**, *812*, 151334. [\[CrossRef\]](#) [\[PubMed\]](#)
55. Silva, M.; Silva, A.; Fernandez-Lodeiro, J.; Casimiro, T.; Lodeiro, C.; Aguiar-Ricardo, A. Supercritical CO₂-Assisted Spray Drying of Strawberry-Like Gold-Coated Magnetite Nanocomposites in Chitosan Powders for Inhalation. *Materials* **2017**, *10*, 74. [\[CrossRef\]](#) [\[PubMed\]](#)

56. Herrero, M.; Castro-Puyana, M.; Mendiola, J.A.; Ibañez, E. Compressed Fluids for the Extraction of Bioactive Compounds. *TrAC Trends Anal. Chem.* **2013**, *43*, 67–83. [[CrossRef](#)]
57. Leme, D.M.; Marin-Morales, M.A. Allium Cepa Test in Environmental Monitoring: A Review on Its Application. *Mutat. Res. Rev. Mutat. Res.* **2009**, *682*, 71–81. [[CrossRef](#)]
58. Frâncica, L.S.; Gonçalves, E.V.; Santos, A.A.; Vicente, Y.S.; Silva, T.S.; Gonzalez, R.S.; Almeida, P.M.; Feitoza, L.L.; Bueno, P.A.A.; Souza, D.C.; et al. Antiproliferative, Genotoxic and Mutagenic Potential of Synthetic Chocolate Food Flavoring. *Braz. J. Biol.* **2022**, *82*, 243628. [[CrossRef](#)] [[PubMed](#)]

Disclaimer/Publisher’s Note: The statements, opinions and data contained in all publications are solely those of the individual author(s) and contributor(s) and not of MDPI and/or the editor(s). MDPI and/or the editor(s) disclaim responsibility for any injury to people or property resulting from any ideas, methods, instructions or products referred to in the content.